The following includes a point-by-point response to the concerns raised by the two reviewers and a description of changes made to the manuscript. Much of this information is repeated from the author's comments, as I was unsure at that time what should be included in which response.

Title choice

Referee comment

> First of all, I think that the title could be slightly different. I do not like the term "remaining" without a date. The title also suggests that you are looking at all the ice shelves in Greenland, but the manuscript does not study Steensby, Ostenfeld, Hagen Brae, Academy or Zachariae Isstrom (I agree that they are much smaller). In addition, the date of the study (2011-2015) should be included in the title.

Author response

We think these are well-made points.

Manuscript changes

We have changed the title to "Satellite-derived submarine melt rates and mass balance (2011–2015) for Greenland's largest remaining ice tongues," qualifying "remaining" with "largest" and adding a date range.

WorldView data description

Referee comment

> Secondly, more details on when exactly the Worldview data were acquired are needed and the authors should explain better how they are merged. The readers know that you use data acquired between 2011 and 2015, but were the images acquired only in years 2011 and 2015, or continuously during the 4/5 years? I believe that Worldview are rather small in coverage. Did the authors rely on different stereo images acquired at different time periods to cover entirely the ice shelves? The authors should provide (could be as supplemental material) a table and maps showing the time tags of the data combined here. They should also state that they assume no change in melt rate between 2011 and 2015.

Author response

As noted in the interactive discussion, we agree with these points. We do mention that the computed values are temporal means, so we don't so much assume no change but instead explicitly report the mean value.

Manuscript changes

We have clarified the method we used to average mass balance estimates (Section 2.3). In order to provide more detail available regarding the images used and the quantity of DEMs generated, we have added a table to the Methodology section with DEM counts, and supplementary material with the exact imagery used. Visualizations portraying the temporal and spatial distributions of our data have also been included as supplementary material.

Mass balance clarifications

Referee comment

> Another point that would need more details is the distinction between surface and submarine melt rates. It would help the readers if the authors add few lines explaining how

> they separate the two, most probably using RACMO2.3. Later in the text (line 6, page 6), the authors estimate the annual mean surface melt rates using RACMO2.3, providing one value per ice shelf. Did the authors compute a single mean value for each ice shelves or did they subtract the mean 2011–2015 map of surface melt (which is not spatially uniform) from the total melt? It would also be interesting to know if the authors used an average surface melt over the period 2011–2015, another period, or directly subtract for each pair of worldview images using the exact surface melt between the two acquisition dates. I agree that this correction might be small compared to submarine melt, but it would definitively give stronger results if this is done and explained properly.

Author response

At the time that this analysis was performed, we had access to the 11 km mass balance product, which does not lend itself to spatially-variable estimates at each ice tongue.

Manuscript changes

We have expanded the manuscript with the following information in Section 2.3:

> The surface component of the mass balance is extracted from the RACMO2.3 [1] model product. We use a single average melt rate computed over the period 2011–2015 for each ice tongue, which is appropriate for mean melt rates computed over multiple years.

Ice and seawater densities

Referee comment

Both reviewers request more information about the densities assumed. Additionally, reviewer 2 writes

> as noted by other users or proponents of this methodology, it may rely (or not) on a few assumptions, including uniform firn density (both spatially and temporally), ice density (idem), and hydrostasy (negligible bridge stresses). You do mention bridge stresses, but seem to gloss over others (e.g. see below). Can you please elaborate on those other assumptions and their eventual impacts on your results?

Author response

This work does not build or incorporate a firn model, and firn properties are assumed stationary in time and space. If significant firn compaction does occur along the ice tongue flow line, our melt rate estimates would tend to over estimate downstream submarine melting, making our conclusions about the concentration of melt at the grounding line stronger.

We make a similar assumption for ice density. Again, densification downstream would result in an increased the melt rate gradient in our estimates. Snow presents a difficulty and prevents us from making conclusions about seasonal melt variations. Averaged over a year or several years density variations from melting or accumulating snow layers are assumed to cancel, which requires there to be no bias introduced by a regular trend in snow depth along the flow line.

Manuscript changes

We have made the constant firn assumption explicit in section 2.5.

To the section 2.3 of the manuscript we have now included and assumed ice column-averaged density of $920\,\mathrm{kg\,m^{-3}}$, and for seawater, $1028\,\mathrm{km\,m^{-3}}$.

The section 2.5 (Errors and Uncertainties) has been amended with the note

> We expect [firn-densification] to be small as the ice tongues considered are well below the equilibrium line and any remaining firn layer is expected to be thin and assumed constant. This is supported by field data described by Dutrieux et al. [2] indicating firn compaction (at PG) to be negligible over a one year period.

Time averages

Referee comment

Reviewer 2 asks,

> how are the time average computed? As the mean of monthly binned differences?

Author response

Time averages are computed by aggregating a monthly means, described in section 2.3.

Manuscript changes

We modify the text to make it clear that we are averaging over monthly means.

> We compute a temporal mean by averaging over average monthly binned estimates of Dh/Dt (January–December) in order to offset bias due to the optical imagery being more available during seasons with more daylight.

As the DEM pairs used extend over multiple months, we weight each month according to the fraction of the month contained within each time span and use the weight to distribute the contribution of each month to submarine melting.

Spatial identification of melt

Referee comment

Reviewer 2 asks

> where is the result from one difference between 2 scenes assumed to reside? At one location between the start and end point, following a streamline? At the starting point? Does that choice impact the end result?

Author response

When calculating the Lagrangian ice thickness change, we simplify by assigning the computed difference to the starting point of the trajectory. In reality, we expect that the melting is distributed over the entire streamline. This information could be used in the averaging and interpolation of melt rates, or a better approximation assigned the melt to some midpoint along the streamline could be made. To estimate the effect that this improvement would have we consider scenarios in the two following contexts:

- a point in the center of Nioghalvfjerdsbræ
- a point near the grounding line of Nioghalvfjerdsbræ

For a central point on Nioghalvfjerdsbræ, a typical surface ice velocity estimated from our data is $650\,\mathrm{m\,yr^{-1}}$. For a one-year temporal baseline, making the alternative extreme assumption, that melt occurs at the downstream location, our estimate in Figure 1 would shift downstream by just over one 512 m pixel. For a point at the grounding line, where surface velocities are closer to $1.3\,\mathrm{km\,yr^{-1}}$, the correction would be approximately two pixels. We think based on these examples that at these scales

the difference in general is not large.

Manuscript changes

We have added a paragraph to section 2.5 describing this source of potentially biased error.

> A source of biased error derives from the assignment of Lagrangian melt rates incurred over a trajectory to a single point. In Figure 1, we assign the melt to the original (upstream) measurement location, which tends to shift the melt estimates slightly upstream in map representations. Based on the ice tongue velocities and temporal baselines used, this upstream bias may be up to approximately 1400 m in the extreme case that all melt actually occurs at the final (downstream) location.

Miscellaneous comments, reviewer 1

Referee comment

> Is it really the submarine melt or total melt including SMB?

Author response

Figure 1 shows our computed submarine melt rates (total melt minus surface melt), i.e. the caption is correct.

Manuscript changes

None.

Referee comment

> The authors mention that the uncertainties on the submarine melt rates are derived from surface elevation. It should also include uncertainties on the SMB. As stated previously, the manuscript would really benefit for a better description on the separation between submarine and surface melt rates.

Author response

I regret to write that in the submitted manuscript and previous author comments, what was treated as the submarine melt uncertainty was in fact the total melt uncertainty. Because of error propagation when combined with surface melt uncertainties, the submarine melt uncertainty is now larger than reported. This has been corrected throughout the manuscript. As a side-effect, because our total melt uncertainty is now computed directly rather than derived from submarine and surface melt rates, our conclusions comparing combined melt rates to grounding line fluxes are slightly strengthened.

In Table 1, the volume fluxes do include estimates of the surface mass balance uncertainty, which is added to the Dh/Dt uncertainty to arrive at the final submarine melt error. This can be made more explicit in the text and caption. The uncertainty chosen ($0.8\,\mathrm{m.w.e\,yr^{-1}}$) at all locations was estimated from Table 4 in [1]. These measurements (made along the K-transect in western Greenland) are far from the ice tongues considered.

Manuscript changes

We have updated the uncertainty estimates and revised the caption on (now) Table 2 to make clear what we report.

Miscellaneous comments, reviewer 2

Referee comment

(Re: reference for claim the velocity is depth-independent)

Manuscript changes

We have added a reference to Weertman [3].

Referee comment

> at the very least you are trying to look at the spatial dis- tribution of melt, so stating that hydrostasy works at the entire ice shelf scale does not really help your case. I understand that quantifying errors resulting from methodolog- ical assumptions is difficult, but you probably don't want to underestimate the impacts of such assumptions.

Author response

Proper quantification of this error is non-trivial and requires an in depth analysis, as the degree to which any portion of the ice tongue is out of hydrostatic equilibrium depends on the spatial scale of thickness variations, the local melt rate history, and period over which the ice has relaxed toward hydrostasy. While not the rigorous analysis that this problem deserves, we could point to modelling in Drews [4] in which they show that under a specific set of circumstances, a $\sim$1 km channel in 280 m thick ice is nearly in balance while a $\sim$1/2 km channel is not.

Manuscript changes

To avoid discounting the possibility for additional error, we add "limitations due to the our assumption of hydrostasy should be kept in mind when considering small-scale features in the results."

Referee comment

(Re: PG pre-calving melt rates)

> This is all rather speculative. And this raises an important point: that of the spatial distribution of melt and its temporal variation, especially if a major change in the geometry like a calving event occurs. Maybe move to the discussion? Or at least attempt to clarify?

Author response

Moving this to the discussion is one possibility, but breaking it up seems to harm readability. Instead, we have rephrased this to de-emphasize it as a result and to ground it in what are safe assumptions.

Manuscript changes

> ...we do not observe submarine melting at PG to be a driver of substantial net volume loss in its current configuration. However, based on a conservative estimate of melting under the former terminus of PG of 5–10 $\mathrm{m\,yr^{-1}}$ and a calved area of approximately 250 $\mathrm{km^2}$, we estimate that the pre-2010 melt flux may have been around 13 $\mathrm{km^3\,yr^{-1}}$ w.e. It is therefore possible that the imbalance between melting and advective replenishment was greater prior to 2010.

Referee comment

(Re: non-independence of draft and slope)

> But is there a cross-correlation between draft and slope? If so (or not), those are not independent parameters, and may be worth noting.

Author response

We agree that this should be noted.

Manuscript changes

We add "Given that draft and slope co-vary" to our discussion.

Referee comment

(Re: channelization and heterogeneity)

> What do you mean by 'heterogeneity'? And also, how do your methodological assumptions impact the channel melt signal? Would you expect it to be smoothed? Enhanced? Can you trust it?

Author response

By heterogeneity, we attempt to summarize results in Sergienko [5] indicating that across-glacier variability in flow and upstream geometry can lead to the development of channels.

Manuscript changes

Our comment here may not add meaningfully to the discussion, and has been replaced with a discussion of methodological limitations.

> Detection of channelization using our methodology is limited by non-hydrostatic behaviour around narrow channels and the potential for drifting snow to accumulate in surface troughs associated with channels, and so those that we do detect tend to be large.

Referee comment

(Re: conclusion)

> Can one use a 4-year record and deduce climatic trends? Shouldn't one expect to see temporal variability of melt? And if so do we know how this melt signal translate to ice dynamics? I would agree that there is a potential for a dynamical response if all things were stable in time, but they probably won't, and you may have sampled a particular time period, or not. So I think readers would benefit from a statement on the numerous possibilities ahead here.

Author response

We absolutely agree on the limitations of a four year record in drawing conclusions about climate, and would like to re-emphasize that these final clauses are speculative based on available data. The dynamical response of the grounding ice sheet to a melt signal is not a satisfactorily resolved question either, resulting in large uncertainties.

Manuscript changes

We have slightly adjusted the conclusion to make it clear that we recognize the limitations in our data for making inferences about climate:

> While our mass deficit estimates are based on an average over a relatively short (4 year) time span, high rates of mass loss lead us to speculate that major changes will take place at 79N in the future as the ice tongue thins and eventually becomes ungrounded at its terminus.

References

[1] B Noël, WJ Van De Berg, E Van Meijgaard, P Kuipers Munneke, R Van De Wal, and MR Van Den Broeke. Evaluation of the updated regional climate model RACMO2.3: summer snowfall impact on the Greenland Ice Sheet. *The Cryosphere*, 9(5):1831–1844, 2015. doi: 10.5194/tc-9-1831-2015.

[2] Pierre Dutrieux, Jan De Rydt, Adrian Jenkins, Paul R. Holland, Ho Kyung Ha, Sang Hoon Lee, Eric J. Steig, Qinghua Ding, E. Povl Abrahamsen, and Michael Schröder. Strong sensitivity of Pine Island ice-shelf melting to climatic variability. *Science*, 343(6167):174–178, 2014. ISSN 0036-8075. doi: 10.1126/science.1244341.

[3] J. Weertman. Deformation of floating ice shelves. *Journal of Glaciology*, 3(21):38–42, 1957. doi: 10.1017/S0022143000024710.

[4] R. Drews. Evolution of ice-shelf channels in Antarctic ice shelves. *The Cryosphere Discussions*, 9 (2):1603–1631, 2015. doi: 10.5194/tcd-9-1603-2015.

[5] O. V. Sergienko. Basal channels on ice shelves. *Journal of Geophysical Research: Earth Surface*, 118(3):13421355, August 2013. ISSN 2169-9003. doi: 10.1002/jgrf.20105.

~~Submarine~~ Satellite-derived submarine melt rates and mass balance (2011–2015) for ~~Greenland'~~Greenland1000s largest remaining ice tongues

Nat Wilson[1,2], Fiammetta Straneo[3], and Patrick Heimbach[4]

[1]MIT-WHOI Joint Program in Oceanography/Applied Ocean Engineering, Cambridge, Massachusetts, USA
[2]Geology and Geophysics Department, Woods Hole Oceanographic Institution, Woods Hole, Massachusetts, USA
[3]Physical Oceanography Department, Woods Hole Oceanographic Institution, Woods Hole, Massachusetts, USA
[4]Jackson School of Geosciences and Institute for Computational Engineering and Sciences, University of Texas at Austin, Austin, Texas, USA

Correspondence to: Nat Wilson (njwilson@mit.edu)

Abstract. Ice shelf-like floating extensions at the termini of Greenland glaciers are undergoing rapid changes with potential implications for the stability of upstream glaciers and the ice sheet as a whole. While submarine melting is recognized as a major contributor to mass loss, the spatial distribution of submarine melting and its contribution to the total mass balance of these floating extensions is incompletely known and understood. Here, we use high-resolution WorldView satellite imagery collected between 2011–2015 to infer the magnitude and spatial variability of melt rates under Greenland's largest remaining ice tongues, Nioghalvfjerdsbræ (79 North Glacier), Ryder Glacier, and Petermann Glacier. Submarine melt rates under the ice tongues vary considerably, exceeding $50\,\mathrm{m\,a^{-1}}$ near the grounding zone and decaying rapidly downstream. Channels, likely originating from upstream subglacial channels, give rise to large melt variations across the ice tongues. We compare the total melt rates to the influx of ice to the ice tongue to assess their contribution to the current mass balance. At Petermann Glacier and Ryder Glacier, we find that the combined submarine and aerial melt approximately balances the ice flux from the grounded ice sheet. At Nioghalvfjerdsbræ the total melt flux ($14.2\pm$~~1.6~~0.96 $\mathrm{km^3\,a^{-1}}$ water-equivalent) exceeds the inflow of ice ($10.2\pm0.59\,\mathrm{km^3\,a^{-1}}$ water-equivalent) indicating present thinning of the ice tongue.

1 Introduction

Mass loss from ice sheets is often greatest at the marine termini (Truffer and Motyka, 2016). Here, ice shelves and ice tongues are hypothesized to influence the stability of the upstream glaciers, and thus of the entire ice sheet (e.g. Dupont and Alley, 2005; Furst et al., 2016). For these reasons, monitoring and understanding processes at marine outlets is key to understanding past and predicting future ice sheet variability.

In Greenland, floating ice tongues currently protrude, or have recently protruded, from the termini of several major outlet glacier systems. However, warming air and ocean temperatures since the mid-1990s have accompanied the reduction or disappearance of most of Greenland's floating ice tongues. This includes the rapid retreat and collapse of the Jakobshavn Isbræ beginning in 1998 (Motyka et al., 2010). Beginning in 2012, the floating ice tongue of Zachariæ Isbræ, one of the largest in

Greenland, has been in a phase of retreat and collapse (Mouginot et al., 2015). Partial loss of the ice tongue has occurred at Petermann Glacier in northwestern Greenland via a series of major calving events (Falkner et al., 2011; Münchow et al., 2014), and Mouginot et al. (2015) and Kjeldsen et al. (2015) have reported thinning at Nioghalvfjerdsbræ in northeast Greenland. In all cases, changes in submarine melting have been identified as the likely driver of these ice tongue changes (e.g. Holland et al., 2008; Motyka et al., 2011; Münchow et al., 2016).

Unfortunately, accurately assessing the submarine melt terms in the mass balance of ice tongues is challenging. This is partly due to the difficulty in making extensive in-situ measurements (Straneo et al., 2012a), and partly due to the trade-offs in spatial and temporal resolution made by existing remote measurement platforms. However, given the recent changes in ice tongues and ice shelves in Greenland and Antarctica and the role they have in buttressing upstream ice flow (Dupont and Alley, 2005), understanding the spatial variability and magnitude of submarine melting is needed to predict future ice sheet variability and sea level rise (Joughin et al., 2012).

We address the observational gap by estimating current melt rates under Greenland's three largest remaining ice tongues: Nioghalvfjerdsbræ (79N), Ryder Glacier (RG), and Petermann Glacier (PG). 79N is the largest existing ice tongue in Greenland by area with a 65 km-long floating ice section confined within a 20 km-wide fjord (Fig. 1) and is grounded at a depth of 700m (Mayer et al., 2000). It is one of three outlet glaciers of the Northeast Greenland Ice Stream (Fahnestock et al., 1993), together with neighbouring Storstrømmen Glacier and Zachariæ Isbræ. While Zachariæ Isbræ has undergone both recent collapse and acceleration, change at 79N has been less visible with no major calving events despite high melt rates first inferred by Mayer et al. (2000). Recently though, several studies have reported that thinning at 79N appears to have taken place during the 21st century (Kjeldsen et al., 2015; Mouginot et al., 2015).

In northwestern Greenland, RG is an ice tongue roughly 25 km long within a 10 km wide fjord and grounded around 500 m depth (Joughin et al., 1999). RG episodically experiences both large calving events and "surge" episodes (Joughin et al., 1996). Further west, PG is the second largest ice tongue in Greenland by area. PG also experiences episodic major calving events (Falkner et al., 2011) with recent examples from 2001, 2008, 2010, and 2012. The grounding line depth at PG is approximately 500 m (Johnson et al., 2011), and rapid basal melting was noted by Rignot (1996). For both 79N and PG, steady state estimates suggest that the ice tongue's mass balance is dominated by submarine melting (Mayer et al., 2000; Johnson et al., 2011; Falkner et al., 2011; Münchow et al., 2014).

Recent estimates of melt rates for these ice tongues are derived from flux gate or flux divergence methods (e.g. Rignot and Steffen, 2008; Enderlin and Howat, 2013). These approaches rely on an assumption of steady state, in which the ice tongue is neither thinning or thickening. Münchow et al. (2014) use ICESat and IceBridge data to show that non-steady melt was important at PG prior to calving. Furthermore, while broad generalizations of the melt rate patterns are currently available from Mayer et al. (2000) and Seroussi et al. (2011) there are no published efforts to carefully map the distribution of melting at 79N and RG over the entire ice tongue.

To address this, we compute Lagrangian hydrostatic ice thickness change over the period 2011–2015 from digital elevation models (DEMs) constructed from WorldView satellite imagery. The results from this analysis allow us to both map the spatial variability of melting and to determine the current ice tongue mass balance. This method has been applied in Antarctica (e.g.

Dutrieux et al., 2013; Moholdt et al., 2014), but never before to Greenland's ice tongues. Contemporary velocity estimates come from optical feature tracking applied to the same imagery used for the elevation models. We combine the material ice thickness change with flow divergence fields to compute the sum of surface and submarine ice tongue melt rates, accounting for dynamic thinning. The surface component of the transient melt, estimated from 0.76–2.0 m of water-equivalent depending on the ice tongue, was extracted from version 2.3 of the Regional Atmospheric Climate Model (RACMO2.3, Noël et al., 2015) and subtracted from the net melt rate to yield estimated submarine melt rates. We present the melt rates as a temporal average over the years for which data are available. Compared to previous approaches that use flux-gate approaches and rely on steady state assumptions, this method more easily incorporates transient thinning or thickening of ice tongues.

2 Methodology

2.1 Data sources and preparation

We used optical image pairs from WorldView-1, WorldView-2, and WorldView-3 satellites, collected over the period 2011–2015 and distributed by the Polar Geospatial Center at the University of Minnesota. We orthorectified these images with the Greenland Ice Mapping Project Digital Elevation Model (Howat et al., 2014) and then constructed new DEMs using the open-source NASA Ames Stereo Pipeline software (Shean et al., 2016). Vertical and horizontal errors in the DEMs are reduced by re-referencing non-glaciated regions to a composite DEM constructed by averaging all available DEMs. Shean et al. (2016) demonstrates that errors in WorldView DEMs are highly correlated, such that co-registration to a common data source removes much of the ~~global~~ relative uncertainty.

Although the accuracy of existing tide models is in most cases unknown, we subtract the tidal elevation predicted from the AOTIM5 tide model (Padman and Erofeeva, 2004). The distance between the most landward edge of the grounding zone and the point where the ice tongue is in hydrostatic equilibrium is on the order of a few kilometers (Brunt et al., 2010). Therefore, the influence of tides will be fully reflected in the ice tongue elevation beyond a narrow buffer zone at the grounding zone, which we exclude from the full analysis (see below). Comparison between the AOTIM5 estimates and a short record collected in 2009 at 79N (G. Hamilton and L. Stearns, personal communication, 2015) reveals an offset in the tide model of approximately 0.2 m.

2.2 Velocity

Over an ice tongue, where basal and lateral stresses are negligible and ice aspect ratio is small, surface velocity is close to the depth-averaged velocity (Weertman, 1957). We compute a grid of correlation offsets by comparing image chips extracted from overlapping hillshaded maps computed from each DEM. We compute the cross-correlation between extracted image chips and then use a Gaussian sub-pixel peak-finding calculation (Debella-Gilo and Kääb, 2011) to estimate displacement. The cross correlation at the peak normalized by the cross correlation standard deviation is retained as a measure of correlation quality. To reduce the area that must be searched for correlation over long temporal baselines, we estimate feature displacement from

the MEaSUReS ice velocity dataset (Joughin et al., 2010) and extract image chips representing a small neighbourhood around these estimates.

2.3 Melt rates

Mass conservation of an ice tongue requires that

$$\frac{\partial h}{\partial t} + \nabla \cdot (\boldsymbol{u} h) = \dot{a}, \tag{1}$$

where h is the ice tongue thickness, $\boldsymbol{u}$ is the depth-averaged velocity, and $\dot{a}$ is the rate of ice thickness change due to combined surface and submarine mass balance. Ice thickness is inferred by assuming hydrostatic equilibrium over the floating ice tongue with a constant ice density of 920 kg m^{-3} and a constant seawater density of 1028 kg m^{-3}. Hydrostasy is a good approximation over sufficiently long horizontal length scales and shallow tongue thickness gradients (Brunt et al., 2010). Immediately downstream of the grounding line the hydrostatic assumption is less justified, so we exclude data within a few kilometers of the grounded ice sheet. The BedMachine mass-conserving bed elevation dataset (Morlighem et al., 2014) serves as a guide to identify where the ice reaches flotation.

The surface component of the mass balance is extracted from the RACMO2.3 (Noël et al., 2015) model product. We use a single average melt rate computed over the period 2011–2015 for each ice tongue, which is appropriate for mean melt rates computed over multiple years.

By neglecting the time derivative in ice thickness, the steady state melt rate can be estimated from the flux divergence alone. For example, Seroussi et al. (2011) and Enderlin and Howat (2013) have applied this method to Greenland's marine terminating glaciers. To include the time derivative in (1) and, in so doing, account for dynamic thickening or thinning of the ice tongue, we compare pairs of ice thickness estimates separated by a temporal baseline. If an Eulerian reference frame is used, this approach is susceptible to temporal aliasing of elevation variations advected along with ice flow. In a Lagrangian framework, temporal aliasing can be avoided as done previously with satellite altimetry data (Moholdt et al., 2014) and stereogrammetric elevation maps (Dutrieux et al., 2013). In this case, the mass balance equation is written in terms of the material time derivative,

$$\frac{Dh}{Dt} + h \nabla \cdot \boldsymbol{u} = \dot{a}. \tag{2}$$

The Lagrangian framework has the additional advantage of avoiding explicit calculation of an ice thickness derivative. Scenes for correlation and melt rate extraction are selected by searching the list of available DEMs for pairs that overlap by minimum of 50 km^2 and that are separated in time by between 180 and 600 days (Table 1). We compute a temporal mean by ~~first binning average~~ averaging over average monthly binned estimates of Dh/Dt ~~by month~~ (January–December) in order to offset bias due to the optical imagery being more available during seasons with more daylight.

2.4 Grounding line fluxes

We estimate the flux of ice from the grounded ice sheet into the floating ice tongue from the correlation-derived ice velocity and ice tongue thickness estimates over a flux-gate at the downstream end of the grounding zone. Retaining the assumption

from above that glacier velocity is invariant with depth, the total grounding line flux Φ is

$$\Phi = \int_a^b \hat{u}(x)h(x)dx, \tag{3}$$

where $\hat{u}$ is the grounding line-normal velocity and limits a and b are as close as possible to the glacier margins. We note that our results are more conservative than other estimates made further upstream, because some ice has melted by the time it crosses the upstream gate.

2.5 Errors and uncertainties

Uncertainty in the time-averaged melt estimates that we derive is due to measurement error, DEM co-registration and correlation errors, errors associated with the tide-corrected ocean elevation, and temporal variability in the ice tongue surface elevation due to accumulation. We make the assumption that these effects are unbiased and attempt to quantify the combined effect of these error sources using a jackknife resampling scheme. This provides uncertainty estimates for the computed melt rates and submarine melt fluxes. As the melt rates are generated from a large number of WorldView DEM pairs, we generate new melt rates by excluding individual DEMs and recomputing the relevant measures using the remaining subset of DEMs. This accounts for sources of random measurement error. Uncertainties reported in the text and figures represent one standard deviation around the computed mean value. Uncertainty in the flux gate volumes is expressed by including the variance from the full set of generated DEMs in the calculation of ice thickness at the flux gate. Some additional error is due to non-random effects such as downstream firn densification, which would yield melt overestimates. We expect this to be small as the ice tongues considered are well below the equilibrium line and any remaining firn layer is expected to be thin and assumed constant. This is supported by field data described by Dutrieux et al. (2014) indicating firn compaction (at PG) to be negligible over a one year period.

A source of biased error derives from the assignment of Lagrangian melt rates incurred over a trajectory to a single point. In Figure 1, we assign the melt to the original (upstream) measurement location, which tends to shift the melt estimates slightly upstream in map representations. Based on the ice tongue velocities and temporal baselines used, this upstream bias may be up to a few kilometers in the extreme case that all melt actually occurs at the final (downstream) location.

The spatial scales at which ice thickness variability (and melt rate variability) may be diagnosed from surface elevation data is physically limited by the melting time scale and ice viscosity. To characterize the accuracy of our ice thickness estimates empirically, we have compared the hydrostatic ice thickness to radar measurements from the MCoRDS echo sounder flown as part of the Operation IceBridge program from 2010–2012 (Leuschen et al., 2010). These data are limited to only a few lines over the ice tongues, but match the ice thickness inferred from the DEMs with a coefficient of determination of 0.93. We expect errors due to non-hydrostatic portions of the ice tongue to be small away from the grounded ice when averaged over coarse grids as in Figure 1 or the entire ice tongue, as in Table 2, however limitations due to the our assumption of hydrostasy should be kept in mind when considering small-scale features in the results.

3 Results

Melt rates for the three ice tongues indicate that the largest melt rates occur near the grounding line (Fig. 1) and decay within 10 km down-glacier from the upstream boundary of our analysis. Maximum melt rates at 79N drop from 50–60 m yr^{-1} near the grounding line to 15 m yr^{-1} 15 km downstream (Fig. 2). Further downstream, melt rates at 79N drop to near zero. Slightly lower grounding zone melt rates are obtained for Petermann (40–50 m yr^{-1}) decreasing to a background rate of 10 m yr^{-1} over a distance of 15–20 km (Fig. 3). At RG, maximum melt rates near the grounding line are similar to those observed at PG; melt rates away from the grounding zone are in the range of 10–20 m yr^{-1} (Fig. 4). These results are qualitatively consistent with aggregated rates obtained by previous studies (e.g. Mayer et al., 2000; Rignot and Steffen, 2008; Münchow et al., 2014).

In addition to this general decrease of melting away from the grounding zone, our results also show smaller scale variations in melt rate on the scale of a few kilometers. At 79N, the fastest melting occurs near the southern two-thirds of the grounding zone and lower along the northern third (Fig. 2). The largest melt rates correspond to the thickest and fastest moving part of the ice stream. Large variability in melt rates in the across-tongue direction are also observed near the grounding zones of RG and PG. In particular, large melt rates (in excess of 50 m yr^{-1}) near the grounding zone of RG occur at the head of an incised channel associated with an elongate 15–20 m depression in surface elevation (Figs. 1, 4). Melt rates on the west side of the grounding zone at RG are much lower in spite of similar ice thickness and draft. Recent bed elevation inversions by Morlighem et al. (2014) indicate that the region of rapid melting identified at RG is at the end of a bedrock trough that reaches over 100 km upstream beneath the Greenland ice sheet. ~~Similarly~~At PG, the melt rates patterns ~~at PG~~ also appear to vary on a scale similar to the channelised geometry of the ice tongue base (Fig. 3), consistent with the broad spatial patterns derived from a steady-state ice flux divergence approach (Rignot and Steffen, 2008) and comparable to radar-derived results (Dutrieux et al., 2014).

The annual surface melt rate predicted at 79N by RACMO2.3 over the period 2011–2015 is 1.5 m a^{-1} water-equivalent (w.e.). Multiplying this by the ice tongue surface area of 1600 km^2 suggests that submarine melting accounts for approximately 80% of the annual non-calving mass loss at 79N. We compute the ice volume flux passing from the grounded ice sheet through the point where the ice tongue becomes hydrostatic to be 10.2±0.59 km^3 yr^{-1} w.e. This may be smaller than the 12±1 km^3 yr^{-1} reported by (Rignot and Steffen, 2008) because of our exclusion of a non-hydrostatic buffer around the actual grounding line. We find that the incoming ice volume is 70% of the observed melt flux within the region considered (14.2±~~1.6~~0.96 km^3 yr^{-1} w.e.), providing direct evidence that the ice tongue is melting at a faster rate than ice is being replenished from upstream (Fig. 5). Excluding calving, the annual net volume loss is 1.3% of the ice tongue's total volume. The imbalance between melting and advective replenishment of ice volume at 79N is consistent with the thinning diagnosed from aerial imagery (Kjeldsen et al., 2015) and by comparing ice thickness derived from radar measurements during the 1990s and the 2010–2014 period (Mouginot et al., 2015).

By contrast, the grounding line flux at RG of 1.9±0.12 km^3 yr^{-1} w.e., slightly smaller than a previously-reported (Rignot et al., 1997) value of 2.3 km^3 yr^{-1}, is not significantly different from the total melt flux (2.1±~~0.21~~0.12 km^3 yr^{-1} w.e.). Similarly, at PG, which lost substantial area from 2001–2012, the present combined observed melt fluxes (11.7±~~1.4~~1.2 km^3 yr^{-1} w.e.) are only slightly larger than the grounding line fluxes (10.8±0.52 km^3 yr^{-1} w.e.). Excluding calving, the annual net volume

loss is 0.4% of the current ice tongue volume. ~~Based~~ As a result, we do not observe submarine melting at PG to be a driver of substantial net volume loss in its current configuration. However, based on a conservative estimate of melting under the former terminus of PG of 5–10 m yr^{-1} and a calved area of approximately 250 km^2, we ~~speculated~~ estimate that the pre-2010 melt flux may have been around 13 km^3 yr^{-1} w.e. ~~As a result, while we do not observe submarine melting at PG to be a driver of substantial net volume loss in its current configuration, it may have been a significant contributor~~ It is therefore possible that the imbalance between melting and advective replenishment was greater prior to 2010.

In all cases, we find a significant correlation between high melt rates and either ice tongue draft ~~and~~ or ice tongue basal slope (Fig. 6). ~~The~~ Given that draft and slope co-vary, it is interesting that the three ice tongues studied above ~~do~~ differ in how the relationship between melt rates and draft/slope is expressed. At 79N, the relationship with slope is perhaps the weakest of the three, with high melt rates inferred even in regions of low basal slope. In general, most of 79N is very low slope, which appears to correspond with the lowest average melt rates of the three glaciers. Given this, the large mass imbalance at 79N is a result of its large area rather than anomalously high average melt rates. In contrast, RG and PG have more similar distributions of basal slope.

4 Discussion

At all ice tongues the highest melt rates are found near the grounding line. This is consistent with the presence of relatively warm, dense waters of Atlantic origins on the nearby continental shelves and fjords (Straneo et al., 2012b). The in-situ temperature of these waters can exceed 1°C at 79N (Wilson and Straneo, 2015), while those at PG in the northwest are consistently measured below 0.5°C (Rignot and Steffen, 2008; Münchow et al., 2016). To our knowledge, no ocean temperatures have been recorded near RG. Nevertheless, profiles collected in 2006 from the continental shelf 150 km away measured maximum temperatures below 300 m near 0.25°C (Steele, 2016). We expect the melt rate at the grounding depth to vary both with the water temperature above the freezing point (the thermal forcing), which in turn varies with pressure, as well with factors that regulate the heat transfer across the ice/ocean boundary layer including ice slope, subglacial discharge (Jenkins, 2011; Straneo and Cenedese, 2015). Assuming that the ocean temperature at the grounding depth is equal to that observed in the fjords (and on the shelf for RG) and equal to 1°C, 0.5°C and 0.25°C for 79N, PG and RG, respectively, and grounding depths of 700 m, 500 m, and 450 m, we estimate the thermal forcing for these three systems to be about 3.4°C, 2.7°C, and 2.5°C. In a broad sense, the melt rates near the grounding zone are consistent with differences in thermal forcing computed at the three ice tongues.

Thermal forcing aside, we also expect higher melting at steeper basal slopes due to the larger entrainment in rising melt water plumes (Little et al., 2009). Again our derived melt rates are largely consistent with this overall pattern but suggest that there is no simple relationship between slope and melt rate.

Our results also indicate that these tongues exhibit a large lateral variability in melt rates due to the presence of basal channels. ~~Channelization is likely derived from heterogeneity in the ice tongue thickness, flow, and oceanic characteristics (Sergienko, 2013)~~Detection of channelization using our methodology is limited by non-hydrostatic behaviour around narrow

channels and the potential for drifting snow to accumulate in surface troughs associated with channels, and so those that we do detect tend to be large. At RG, the deep central channel along the base of the ice tongue appears to be a product of high melt rates, and may also concentrate them in a positive feedback. The lower advection rates at RG may also make it more susceptible to developing deep channels, as the rate of replenishment of ice from upstream is lower. At PG, ice advection rates at the grounding line are similar to 79N, and so the presence of deep channels must be due to either more intense grounding line melting or more active maintenance by submarine melting along the length of the ice tongue (e.g. Gladish et al., 2012).

5 Conclusions

Our results highlight high spatial heterogeneity in melt rates beneath Greenland's ice tongues in both the along-flow and the across-flow directions. This latter component of spatial variability is typically ignored in models, but is likely to be important to accurately predict ice tongue and buttressing sensitivities to ocean temperature and ice geometry changes. We also show that PG and RG are in their current geometries close to maintaining their total volume, with grounding line influxes balancing inferred melting. We find that in spite of apparently minor changes in surface area in recent decades at 79N, net mass losses there are the highest of the remaining large ice tongues in Greenland. ~~We~~ While our mass deficit estimates are based on an average over a relatively short (4 year) time span, high rates of mass loss lead us to speculate that major changes will take place at 79N in the future as the ice tongue thins and eventually becomes ungrounded at its terminus. This ~~potentially has~~ could have important implications for buttressing of the inland portion of the outlet glacier that is the exit of the Northeast Greenland Ice Stream.

Code and data availability. The satellite data used in this research are available subject to the data licensing requirements of the Polar Geospatial Research Center. Lists of the images used will be provided upon request. Code used to analyze the satellite images is available publicly at https://bitbucket.org/njwilson23/worldview_processing or upon request.

Author contributions. NW developed the code, performed the WorldView data analysis, and was the primary contributor to the text of the manuscript. FS actively contributed ideas and also submitted text in the manuscript. PH provided guidance by contributing helpful advice on the scientific ideas and feedback on the manuscript.

Competing interests. The authors are not aware of any competing financial interests.

Acknowledgements. NW, FS, and PH were supported by NASA NNX13AK88G and NSF OCE 1434041. WorldView-1/2/3 imagery were made available by the Polar Geospatial Center at the University of Minnesota and DigitalGlobe. Gordon Hamilton and Leigh Stearns provided

GPS data from 79N. RACMO2.3 data were kindly made available by M. R. van den Broeke. David Shean contributed helpful advice and discussion regarding processing WorldView imagery with the NASA Ames Stereo Pipeline.

References

Brunt, K. M., Fricker, H. A., Padman, L., Scambos, T. A., and O'Neel, S.: Mapping the grounding zone of the Ross Ice Shelf, Antarctica, using ICESat laser altimetry, Annals of Glaciology, 51, 71–79, doi:10.3189/172756410791392790, 2010.

Debella-Gilo, M. and Kääb, A.: Sub-pixel precision image matching for measuring surface displacements on mass movements using normalized cross-correlation, Remote Sensing of Environment, 115, 130–142, doi:10.1016/j.rse.2010.08.012, 2011.

Dupont, T. K. and Alley, R. B.: Assessment of the importance of ice-shelf buttressing to ice-sheet flow, Geophysical Research Letters, 32, doi:10.1029/2004gl022024, 2005.

Dutrieux, P., Vaughan, D. G., Corr, H. F. J., Jenkins, A., Holland, P. R., Joughin, I., and Fleming, A. H.: Pine Island Glacier ice shelf melt distributed at kilometre scales, The Cryosphere, 7, 1543–1555, doi:10.5194/tc-7-1543-2013, 2013.

Dutrieux, P., De Rydt, J., Jenkins, A., Holland, P. R., Ha, H. K., Lee, S. H., Steig, E. J., Ding, Q., Abrahamsen, E. P., and Schröder, M.: Strong Sensitivity of Pine Island Ice-Shelf Melting to Climatic Variability, Science, 343, 174–178, doi:10.1126/science.1244341, 2014.

Enderlin, E. M. and Howat, I. M.: Submarine melt rate estimates for floating termini of Greenland outlet glaciers (2000–2010), Journal of Glaciology, 59, 67–75, doi:10.3189/2013JoG12J049, 2013.

Fahnestock, M., Bindschadler, R., Kwok, R., and Jezek, K.: Greenland ice sheet surface properties and ice dynamics from ERS-1 SAR imagery, Science, 262, 1530–1534, doi:10.1126/science.262.5139.1530, 1993.

Falkner, K. K., Melling, H., Münchow, A. M., Box, J. E., Wohlleben, T., Johnson, H. L., Gudmandsen, P., Samelson, R., Copland, L., Steffen, K., Rignot, E., and Higgins, A. K.: Context for the recent massive Petermann Glacier calving event, Eos, 92, 117–118, doi:10.1029/2011EO140001, 2011.

Furst, J. J., Durant, G., Gillet-Chaulet, F., Tavard, L., Rankl, M., and Gagliardini, O.: The safety band of Antarctic ice shelves, Nature Climate Change, 6, 479–482, doi:10.1038/nclimate2912, 2016.

Gladish, C. V., Holland, D. M., Holland, P. R., and Price, S. F.: Ice-shelf basal channels in a coupled ice/ocean model, Journal of Glaciology, 58, 1227–1244, doi:10.3189/2012JoG12J003, 2012.

Holland, D. M., Thomas, R. H., De Young, B., Ribergaard, M. H., and Lyberth, B.: Acceleration of Jakobshavn Isbræ triggered by warm subsurface ocean waters, Nature Geoscience, 1, 659–664, doi:10.1038/ngeo316, 2008.

Howat, I. M., Negrete, A., and Smith, B. E.: The Greenland Ice Mapping Project (GIMP) land classification and surface elevation datasets, The Cryosphere, 8, 1509–1518, doi:10.5194/tc-8-1509-2014, 2014.

Jenkins, A.: Convection-Driven Melting near the Grounding Lines of Ice Shelves and Tidewater Glaciers, Journal of Physical Oceanography, 41, doi:10.1175/JPO-D-11-03.1, 2011.

Johnson, H. L., Münchow, A., Falkner, K. K., and Melling, H.: Ocean circulation and properties in Petermann Fjord, Greenland, Journal of Geophysical Research: Oceans (1978–2012), 116, doi:10.1029/2010JC006519, 2011.

Joughin, I., Tulaczyk, S., Fahnestock, M., and Kwok, R.: A mini-surge on the Ryder Glacier, Greenland, observed by satellite radar interferometry, Science, 274, 228–230, doi:10.1126/science.274.5285.228, 1996.

Joughin, I., Fahnestock, M., Kwok, R., Gogineni, P., and Chris, A.: Ice flow of Humboldt, Petermann and Ryder Gletscher, northern Greenland, Journal of Glaciology, 45, 231–241, doi:10.3198/1999JoG45-150-231-241, 1999.

Joughin, I., Smith, B. E., Howat, I. M., Scambos, T., and Moon, T.: Greenland flow variability from ice-sheet-wide velocity mapping, Journal of Glaciology, 56, doi:10.3189/002214310792447734, 2010.

Joughin, I., Alley, R. B., and Holland, D. M.: Ice-sheet response to oceanic forcing, Science, 338, 1172–1176, doi:10.1126/science.1226481, 2012.

Kjeldsen, K. K., Korsgaard, N. J., Björck, A. A., Khan, S. A., Box, J. E., Funder, S., Larsen, N. K., Bamber, J. L., Colgan, W., van den Broecke, M. R., Siggard-Andersen, M.-L., Nuth, C., Schomacker, A., Andresen, C. S., Willerslev, E., and Kjær, K. H.: Spatial and temporal distribution of mass loss from the Greenland Ice Sheet since AD 1900, Nature Letters, 528, 396–400, doi:10.1038/nature16183, 2015.

Leuschen, C., Gogineni, P., F., R.-M., Paden, J., and C., A.: IceBridge MCoRDS L2 Ice Thickness, Version 1., National Snow and Ice Data Center Distributed Active Archive Center, doi:10.5067/GDQ0CUCVTE2Q, http://nsidc.org/data/irmcr2, accessed 12 June 2016, 2010.

Little, C. M., Gnanadesikan, A., and Oppenheimer, M.: How ice shelf morphology controls basal melting, Journal of Geophysical Research, 114, C12 007, doi:10.1029/2008JC005197, 2009.

Mayer, C., Reeh, N., Jung-Rothenhäusler, F., Huybrechts, P., and Oerter, H.: The subglacial cavity and implied dynamics under Nioghalvfjerdsfjorden Glacier, NE-Greenland, Geophysical Research Letters, 27, 2289–2292, doi:10.1029/2000GL011514, 2000.

Moholdt, G., Padman, L., and Fricker, H. A.: Basal mass budget of Ross and Filchner-Ronne ice shelves, Antarctica, derived from Lagrangian analysis of ICESat altimetry, Journal of Geophysical Research: Earth Surface, 119, 2361—-2380, doi:10.1002/2014JF003171, 2014.

Morlighem, M., Rignot, E., Mouginot, J., Seroussi, H., and Larour, E.: Deeply incised submarine glacial valleys beneath the Greenland ice sheet, Nature Geoscience, 7, doi:10.1038/ngeo2167, 2014.

Motyka, R. J., Fahnestock, M., and Truffer, M.: Volume change of Jakobshavn Isbræ, West Greenland: 1985–1997–2007, Journal of Glaciology, 56, 635–646, doi:10.3189/002214310793146304, 2010.

Motyka, R. J., Truffer, M., Fahnestock, M., Mortensen, J., Rysgaard, S., and Howat, I.: Submarine melting of the 1985 Jakobshavn Isbræ floating tongue and the triggering of the current retreat, Journal of Geophysical Research: Earth Surface, 116, doi:10.1029/2009JF001632, 2011.

Mouginot, J., Rignot, E., Scheuchl, B., Fenty, I., Khazendar, A., Morlighem, M., Buzzi, A., and Paden, J.: Fast retreat of Zachariæ Isstrøm, northeast Greenland, Science, 350, 1357–1361, doi:10.1126/science.aac7111, 2015.

Münchow, A., Padman, L., and Fricker, H. A.: Interannual changes of the floating ice shelf of Petermann Gletscher, North Greenland from 2000 to 2012, Journal of Glaciology, 60, doi:10.3189/2014JoG13J135, 2014.

Münchow, A., Padman, L., Washam, P., and Nicholls, K. W.: The ice shelf of Petermann Gletscher, North Greenland and its connection to the Arctic and Atlantic oceans, Oceanography, doi:10.5670/oceanog.2016.101, 2016.

Noël, B., Van De Berg, W., Van Meijgaard, E., Kuipers Munneke, P., Van De Wal, R., and Van Den Broeke, M.: Evaluation of the updated regional climate model RACMO2.3: summer snowfall impact on the Greenland Ice Sheet, The Cryosphere, 9, 1831–1844, doi:10.5194/tc-9-1831-2015, 2015.

Padman, L. and Erofeeva, S.: A barotropic inverse tidal model for the Arctic Ocean, Geophysical Research Letters, 31, doi:10.1029/2003GL019003, l02303, 2004.

Rignot, E.: Tidal motion, ice velocity and melt rate of Petermann Gletscher, Greenland, measured from radar interferometry, Journal of Glaciology, 42, 476–485, doi:10.3198/1996JoG42-142-476-485, 1996.

Rignot, E. and Steffen, K.: Channelized bottom melting and stability of floating ice shelves, Geophysical Research Letters, 35, doi:10.1029/2007GL031765, 2008.

Rignot, E. J., Gogineni, S. P., Krabill, W. B., and Ekholm, S.: North and Northeast Greenland Ice Discharge from Satellite Radar Interferometry, Science, 276, 934–937, doi:10.1126/science.276.5314.934, http://science.sciencemag.org/content/276/5314/934, 1997.

Sergienko, O. V.: Basal channels on ice shelves, Journal of Geophysical Research: Earth Surface, 118, 1342–1355, doi:10.1002/jgrf.20105, 2013.

Seroussi, H., Morlighem, M., Rignot, E., Larour, E., Aubry, D., Dhia, H. B., and Kristensen, S. S.: Ice flux divergence anomalies on 79north Glacier, Greenland, Geophysical Research Letters, 38, L09 501, doi:10.1029/2011GL047338, 2011.

Shean, D. E., Alexandrov, O., Moratto, Z. M., Smith, B. E., Joughin, I. R., Porter, C., and Morin, P.: An automated, open-source pipeline for mass production of digital elevation models (DEMs) from very-high-resolution commercial stereo satellite imagery, ISPRS Journal of Photogrammetry and Remote Sensing, 116, 101–117, doi:10.1016/j.isprsjprs.2016.03.012, 2016.

Steele, M.: Arctic Freshwater Switchyard Project: Spring temperature and Salinity data collected by aircraft in the Arctic Ocean, May 2006 – May 2007 (NODC Accession 0057319), NODC, version 1.1, gov.noaa.nodc:0057319, accessed 2016 October 10, 2016.

Straneo, F. and Cenedese, C.: The Dynamics of Greenland's Glacial Fjords and Their Role in Climate, Annual Review of Marine Science, 7, 89–112, doi:10.1146/annurev-marine-010213-135133, 2015.

Straneo, F., Sergienko, O., Heimbach, P., and Hamilton, G.: U.S. CLIVAR: Climate Variability and Predictibility, White Paper 2012-2, U.S. CLIVAR Working Group on Greenland and Ice Sheet-Ocean Interactions (GRISO), Washington, DC, 2012a.

Straneo, F., Sutherland, D. A., Holland, D., Gladish, C., Hamilton, G. S., Johnson, H. L., Rignot, E., Xu, Y., and Koppes, M.: Characteristics of ocean waters reaching Greenland's glaciers, Annals of Glaciology, 53, 202–210, doi:10.3189/2012AoG60A059, 2012b.

Truffer, M. and Motyka, R. J.: Where glaciers meet water: Subaqueous melt and its relevance to glaciers in various settings, Reviews of Geophysics, 54, 220–239, doi:10.1002/2015RG000494, 2015RG000494, 2016.

Weertman, J.: Deformation of Floating Ice Shelves, Journal of Glaciology, 3, 38–42, doi:10.1017/S0022143000024710, 1957.

Wilson, N. J. and Straneo, F.: Water exchange between the continental shelf and the cavity beneath Nioghalvfjerdsbræ (79 North Glacier), Geophysical Research Letters, 42, doi:10.1002/2015GL064944, 2015GL064944, 2015.

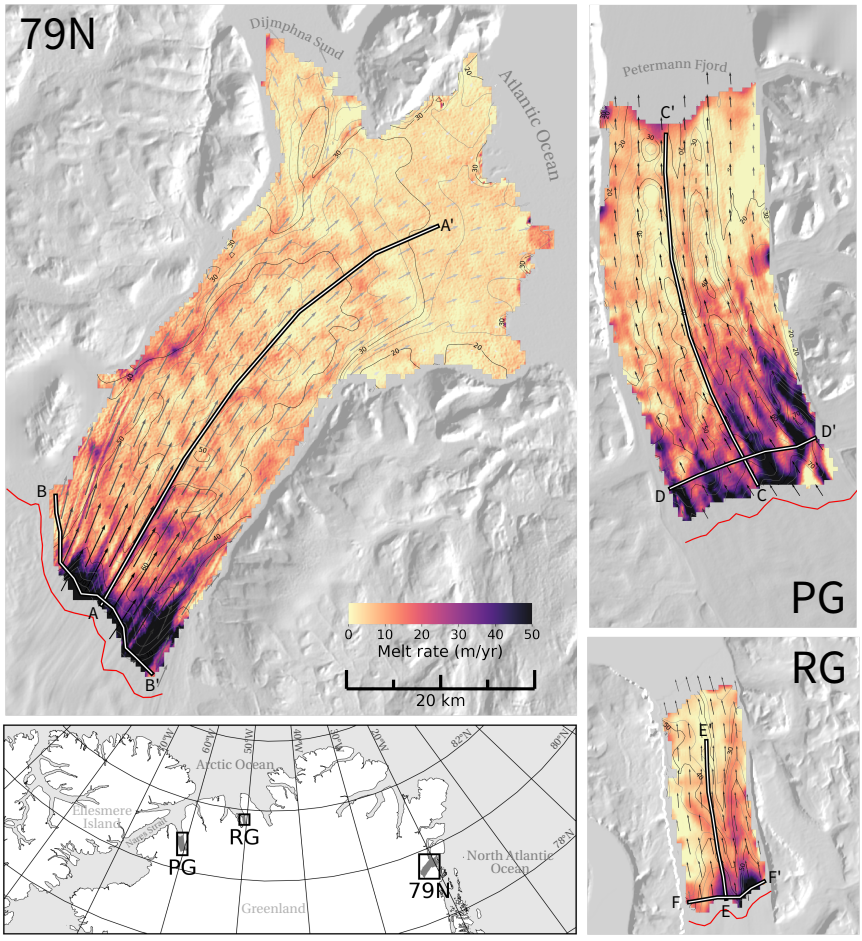

Figure 1. Map of submarine melt rates from Greenland's major ice tongues derived from WorldView satellite DEMs. The colour shading shows regions of rapid submarine melting, while the arrows indicate ice flow directions. Red line approximates the grounding line. Inset map in the lower left provides regional context.

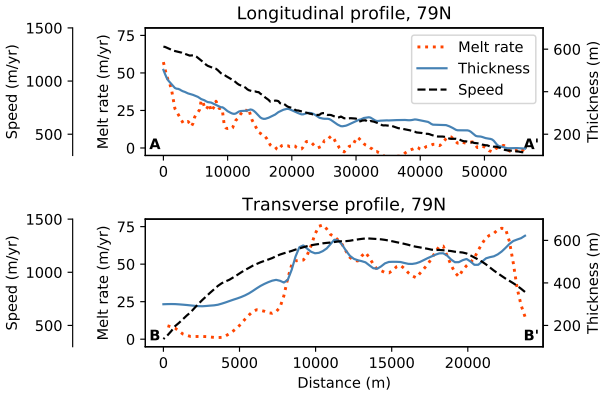

Figure 2. Velocity, melt rate, and ice thickness profiles for 79N. Longitudinal profile along the glacier centreline. Transverse profile is taken approximately 1 km downstream of the upstream flux gate.

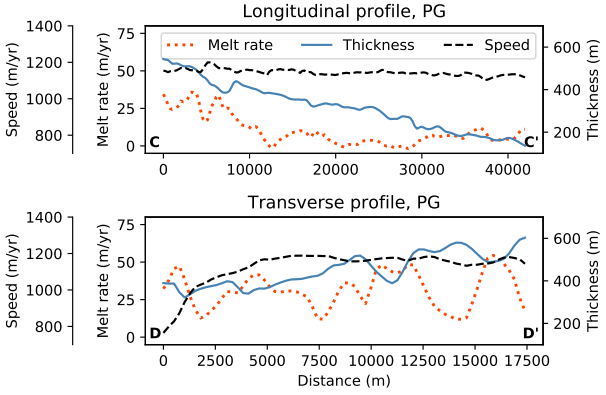

Figure 3. Velocity, melt rate, and ice thickness profiles for PG. Longitudinal profile is outside of a long sub-shelf channel. Transverse profile is taken approximately 1 km downstream of the upstream flux gate.

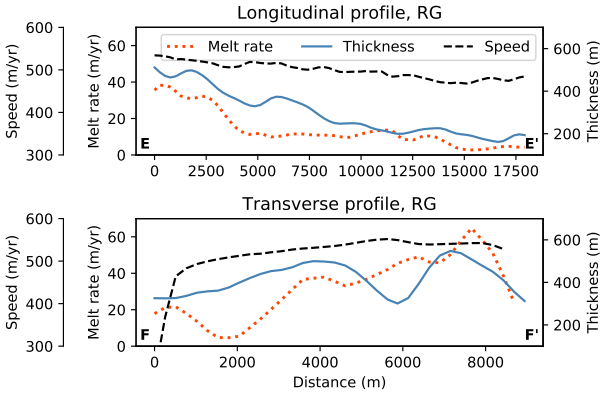

Figure 4. Velocity, melt rate, and ice thickness profiles for RG. Longitudinal profile computed along a transect to the west of the major sub-shelf channel. Transverse profile is taken approximately 1 km downstream of the upstream flux gate.

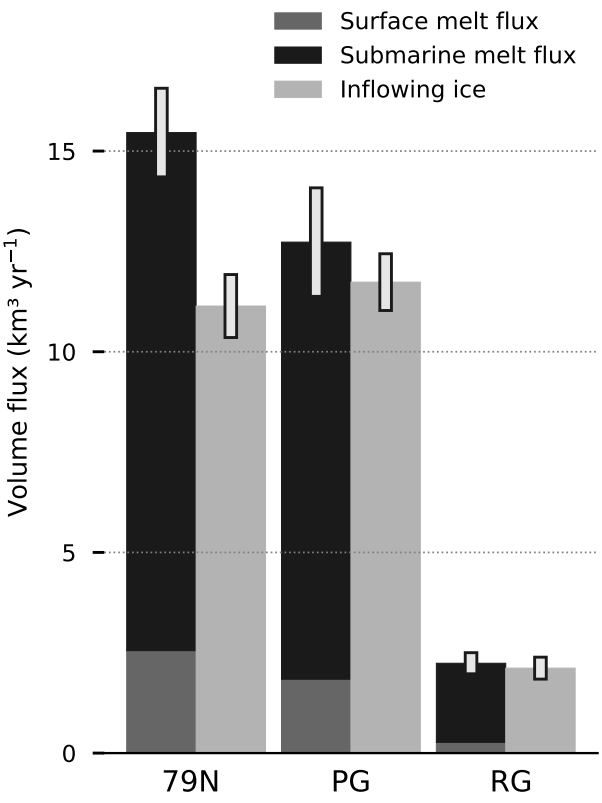

Figure 5. Comparison of ice volume fluxes. Melt flux and grounding line volume flux for each floating ice tongue are shown, with melt fluxes partitioned between submarine and subaerial components. Error bars represent one standard deviation above and below the estimate.

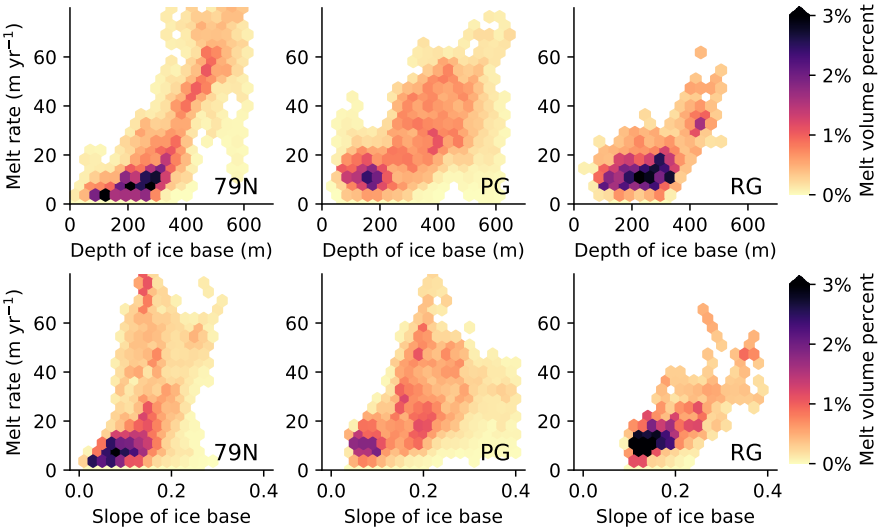

Figure 6. Relationships between estimated melt rates and the depth and slope of the ice tongue base. Shading serves as a visual guide to the density of observations in each cell.

Table 1. ~~**Volume fluxes**~~ **Digital Elevation Model (DEM) counts** Counts of DEMs used for ~~Greenland's major~~ each ice ~~tongues~~tongue, ~~in freshwater equivalent.Ranges on submarine melt flux are one standard deviation and derive from surface~~ combined with counts of DEM pairs used for elevation ~~uncertainty~~differencing.

Glacier	DEM count	DEM pair count
79N	108	915
RG	36	211
PG	97	751

Table 2. Volume fluxes for Greenland's major ice tongues, in freshwater equivalent. Total melt flux uncertainties are one standard deviation around measurements described here. Surface melt flux uncertainty is estimated from (Noël et al., 2015). Submarine melt flux uncertainty is derived from total and surface melt flux uncertainty.

Glacier	Volume km^3	Inflowing ice $km^3\ yr^{-1}$	~~Submarine~~ Total melt flux $km^3\ yr^{-1}$	Surface melt flux $km^3\ yr^{-1}$	Submarine melt flux $km^3\ yr^{-1}$
79N	314	10.2±0.59	~~11.9~~14.2±0.96	2.3±1.3	11.9±1.6
RG	51.0	1.9±0.12	~~1.8~~2.0±0.12	0.25±0.17	1.8±0.21
PG	215	10.8±0.52	~~10.0~~11.7±1.2	1.7±0.68	10.0±1.4